



Physiologically-based pharmacokinetic model to investigate the effect of pregnancy on risperidone and paliperidone pharmacokinetics: Application to a pregnant woman and her neonate

Mahdy, Walaa Y. B. ; Yamamoto, Kazuhiro ; Ito, Takahiro ; Fujiwara, Naoko ; Fujioka, Kazumichi ; Horai, Tadasu ; Otsuka, Ikuo ; Imafuku,...

(Citation)

Clinical and Translational Science, 16(4):618-630

(Issue Date)

2023-04

(Resource Type)

journal article

(Version)

Version of Record

(Rights)

© 2023 The Authors. Clinical and Translational Science published by Wiley Periodicals LLC on behalf of American Society for Clinical Pharmacology and Therapeutics. This is an open access article under the terms of the Creative Commons Attribution-NonCommercial License, which permits use, distribution and reproduction in any mediu...

(URL)

<https://hdl.handle.net/20.500.14094/0100481856>





ARTICLE

Physiologically-based pharmacokinetic model to investigate the effect of pregnancy on risperidone and paliperidone pharmacokinetics: Application to a pregnant woman and her neonate

Walaa Y. B. Mahdy¹ | Kazuhiro Yamamoto^{1,2} | Takahiro Ito² |
Naoko Fujiwara² | Kazumichi Fujioka³ | Tadasu Horai⁴ | Ikuo Otsuka⁴ |
Hitomi Imafuku⁵ | Tomohiro Omura^{1,2} | Kazumoto Iijima³ | Ikuko Yano^{1,2}

¹Department of Pharmaceutics,
Kobe University Graduate School of
Medicine, Kobe, Japan

²Department of Pharmacy, Kobe
University Hospital, Kobe, Japan

³Department of Pediatrics, Kobe
University Graduate School of
Medicine, Kobe, Japan

⁴Department of Psychiatry, Kobe
University Graduate School of
Medicine, Kobe, Japan

⁵Department of Obstetrics and
Gynecology, Kobe University Graduate
School of Medicine, Kobe, Japan

Correspondence

Kazuhiro Yamamoto, Department of
Pharmacy, Kobe University Hospital,
7-5-2 Kusunoki-cho, Chuo-ku, Kobe
650-0017, Japan.

Email: yamakz@med.kobe-u.ac.jp

Abstract

This study aimed to determine the effects of pregnancy and ontogeny on risperidone and paliperidone pharmacokinetics by assessing their serum concentrations in two subjects and constructing a customized physiologically-based pharmacokinetic (PBPK) model. Risperidone and paliperidone serum concentrations were determined in a pregnant woman and her newborn. PBPK models for risperidone and paliperidone in adults, pediatric, and pregnant populations were developed and verified using the Simcyp simulator. These models were then applied to our two subjects, generating their “virtual twins.” Effects of pregnancy on both drugs were examined using models with fixed pharmacokinetic parameters. In the neonatal PBPK simulation, 10 different models for estimating the renal function of neonates were evaluated. Risperidone was not detected in the serum of both pregnant woman and her newborn. Maternal and neonatal serum paliperidone concentrations were between 2.05–3.80 and 0.82–1.03 ng/ml, respectively. Developed PBPK models accurately predicted paliperidone's pharmacokinetics, as shown by minimal bias and acceptable precision across populations. The individualized maternal model predicted all observed paliperidone concentrations within the 90% prediction interval. Fixed-parameter simulations showed that CYP2D6 activity largely affects risperidone and paliperidone pharmacokinetics during pregnancy. The Flanders metadata equation showed the lowest absolute bias (mean error: $22.3\% \pm 6.0\%$) and the greatest precision (root mean square error: 23.8%) in predicting paliperidone plasma concentration in the neonatal population. Our constructed PBPK model can predict risperidone and paliperidone pharmacokinetics in pregnant and neonatal populations, which could help with precision dosing using the PBPK model-informed approach in special populations.

This is an open access article under the terms of the [Creative Commons Attribution-NonCommercial](https://creativecommons.org/licenses/by-nc/4.0/) License, which permits use, distribution and reproduction in any medium, provided the original work is properly cited and is not used for commercial purposes.

© 2023 The Authors. *Clinical and Translational Science* published by Wiley Periodicals LLC on behalf of American Society for Clinical Pharmacology and Therapeutics.

Study Highlights

WHAT IS THE CURRENT KNOWLEDGE ON THE TOPIC?

Risperidone and paliperidone are second-generation antipsychotics commonly used to treat psychosis. Due to ethical and legal concerns, pregnant women and children are typically excluded from clinical research. Consequently, there is a dearth of data on the doses, pharmacokinetics, and safety of risperidone and paliperidone during pregnancy, and neonatal periods. Thus, mechanistic pharmacokinetic modeling that can predict drug pharmacokinetics and optimize dosing regimens is essential for these vulnerable populations.

WHAT QUESTION DID THIS STUDY ADDRESS?

This study aimed to provide viable insights into risperidone and paliperidone serum concentrations in a Japanese pregnant woman and her neonate, demonstrating the feasibility of a physiologically-based pharmacokinetic (PBPK) model in predicting various pharmacokinetic parameters in individual patients along with evaluating several pharmacokinetic changes associated with pregnancy and their effects on drug disposition. Finally, determination of the most accurate estimated glomerular filtration rate (eGFR) model for predicting neonatal paliperidone clearance.

WHAT DOES THIS STUDY ADD TO OUR KNOWLEDGE?

Our study has three main implications: (1) laying out a strategy for using PBPK to predict drug disposition in an individual patient with limited plasma samples; (2) identifying key parameters that influence drug pharmacokinetic parameters in pregnant women; and (3) comparing various maturation models and formulas for calculating eGFR in our newborn.

HOW MIGHT THIS CHANGE CLINICAL PHARMACOLOGY OR TRANSLATIONAL SCIENCE?

As part of model-informed precision dosing, this validated PBPK model can be utilized to optimize risperidone and paliperidone dose regimens for individual pregnant and pediatric patients.

INTRODUCTION

Most mental illnesses in women arise throughout their reproductive years, especially during the perinatal period, and the rate of antipsychotic use during pregnancy has nearly doubled in the last decade.¹ Prior to the coronavirus disease 2019 (COVID-19) pandemic, researchers had estimated that roughly 20% of pregnant women might acquire a mental illness.² Considering its detrimental toll, recent studies show that the COVID-19 pandemic has further inflamed perinatal mental health problems.³ Risperidone (RIS) is one of the most commonly prescribed second-generation antipsychotic drugs⁴ for managing schizophrenia and bipolar disorder. Although the actual number of women who have been exposed to RIS during pregnancy is unknown, roughly 23% of all antipsychotic prescriptions for pregnant women between 2001 and 2007 contained RIS.⁵ Although animal studies have demonstrated that RIS does not cause direct reproductive toxicity or teratogenic effects,⁶ human case studies have shown that RIS may cause significant unwanted effects, ranging from self-limiting side effects to

newborns requiring intensive care and prolonged hospitalization.^{7,8} Therefore, RIS prescriptions for pregnant women are restricted to circumstances in which the benefits outweigh the risks to the fetus.⁷

After oral administration, RIS is nearly completely absorbed from the gastrointestinal tract, with peak plasma concentrations at 1–2 h.⁹ Many medications, including RIS, are metabolized by cytochrome P450 2D6 (CYP2D6).⁴ In humans, the main metabolic pathway for RIS is the synthesis of its active metabolite, 9-hydroxyrisperidone (9-OH-RIS [paliperidone]), through CYP2D6 and, to a lesser extent, cytochrome P450 3A4 (CYP3A4).⁴ In contrast, paliperidone (PAL), a medication used to treat certain mental and mood disorders, undergoes negligible hepatic biotransformation by CYP2D6 and is primarily eliminated via the kidneys.¹⁰ In therapeutic plasma concentrations, 89% of RIS and 79% of PAL are mostly bound to serum albumin.^{11,12} Anatomic, physiologic, and metabolic changes during pregnancy can impact the absorption, distribution, metabolism, and excretion (ADME) of these medications. According to a previous clinical study,¹³ pregnant women have lower RIS

active moiety (AM; RIS + PAL) levels compared with non-pregnant women. However, the specific process by which pregnant women's serum levels of RIS differ from those of non-pregnant women remains unclear.

Pregnant women and newborns are often excluded from scientific studies due to ethical and legal concerns.¹⁴ Consequently, current knowledge on optimal dosing regimens, pharmacokinetics, and safety characteristics of various drugs during pregnancy, fetal, and neonatal periods is inadequate.¹⁴ Physiologically-based pharmacokinetic (PBPK) modeling, which incorporates drug-specific parameters (e.g., physicochemical and disposition characteristics), physiological parameters relevant to ADME processes, and clinical trial designs to generate a quantitative predictive model,¹⁵ might be a feasible approach for optimizing dosing regimens in pregnant and pediatric populations. A promising novel method for precise drug dosing has evolved by matching the unique characteristics of real-life patients to those of their “virtual twins.”¹⁵ These attributes include intrinsic (age, sex, physical traits, kidney and liver function, race, and genetic background) and extrinsic variables (comedication, smoking, and fasting).¹⁵ The “virtual twins” approach allows researchers to shift PBPK implementations from population-based to precision dosing for individual patients.

Glomerular filtration rate (GFR) is an index that reflects renal function, which changes rapidly with age and growth in children, especially neonates.¹⁶ The characterization of neonatal renal maturation allows for a more precise initial dosage regimen in pediatric clinical trials that contain medications cleared by the kidneys, such as vancomycin and amikacin.¹⁷ Numerous models have been constructed to characterize the developmental changes in GFR,^{17–26} however, much uncertainty still exists over the optimal approach for estimating renal function and determining GFR in newborns.

Thus, the objectives of this study were to develop, verify, and personalize pediatric and pregnant PBPK models for RIS and PAL. Consequently, this personalized version was used for the assessment of RIS and PAL pharmacokinetics in a Japanese pregnant woman and her newborn by utilizing the “virtual twin” approach. Moreover, we assessed the effects of neonatal renal function estimation methods on newborn pharmacokinetics using the PBPK model approach.

MATERIALS AND METHODS

Blood sampling and measurement of RIS and PAL concentrations

Routine time-series serum samples were collected from a Japanese pregnant woman and her newborn baby. Serum

RIS and PAL concentrations were measured by liquid chromatography–tandem mass spectrometry (LC–MS/MS; LC–MS-8030; Shimadzu, Kyoto, Japan). Detailed information is shown in the [Supplementary Materials](#).

Development of RIS and PAL PBPK models

The PBPK models were built using the Simcyp ADME simulator, version 21 (Certara UK Limited, Simcyp Division, Sheffield, UK). WebPlotDigitizer version 4.21²⁷ was used to digitize clinical plasma data from figures published in scientific papers and Rstudio version 1.4.1106 to construct the goodness-of-fit (GOF) plots.

The following stages summarize the basic approach used to construct and verify the RIS and PAL PBPK models. [Figure S1](#) demonstrates the workflow of the PBPK model development for RIS and PAL. In step 1, preliminary data from literature was used to build the PBPK models. These data were gathered from both in vitro^{28,29} and in vivo clinical pharmacokinetic^{10,30–32} studies following intravenous (i.v.) and oral doses ([Tables S1](#) and [S2](#)). In step 2, the model was verified by comparing the simulated pharmacokinetic data with data obtained from published clinical trials in White and Japanese patients.^{13,31–36} [Table S3](#) summarizes these clinical trials, which were divided into two datasets, one for model development and one for model verification, including their study characteristics and dosage regimens. In step 3, the verified adult PBPK model was extrapolated to the pediatric population, and it was then verified by comparing the simulated pharmacokinetic data to the observed clinical data from White pediatric clinical trials involving multiple oral dosages.³⁵ Additionally, by parameterizing and expanding the model structure to pregnancy-induced physiological changes, the adult (non-pregnant) PBPK model for RIS and PAL was extrapolated to the pregnancy population. Then, it was utilized to estimate AM plasma concentrations at baseline (pregnancy week 0) and by trimester during pregnancy in four pregnant patients with nine sampling points at baseline, and five sampling points in each pregnancy trimester.¹³ These virtual populations were based on patient characteristics of the included clinical trials. All drug-dependent parameters were held constant at the adult PBPK model values. Finally, in step 4, the final pediatric and pregnant PBPK models were individualized and used to predict the serum disposition of RIS and PAL in two subjects, a Japanese woman and her newborn. Simcyp libraries, including “sim-healthy volunteers,” “sim-pediatrics,” and “sim-pregnant,” were used to derive population-dependent physiological parameters in human PBPK models. The development of the RIS and PAL PBPK models is shown in detail in the [Supplementary Materials](#).

Description of the two subjects

A 38-year-old pregnant Japanese woman had mental health issues and had been receiving psychotherapy for a long duration. The antipsychotic therapy was discontinued when the subject began taking medications to conceive. During the third trimester, she had a panic episode that necessitated hospitalization with RIS 0.5 mg twice daily until the day of birth (12 days in total). After 40 weeks and 5 days of gestation, a male baby was born vaginally. No evidence of congenital malformations or neonatal abstinence syndrome was observed at birth. After delivery, the patient continued to take RIS, but the dosage was changed to 1 mg once daily from day 1 postpartum. The mother was discharged from the hospital and continued to take the medication at home for 2 additional days. The mother's weight was 55.1 kg before childbirth, and her height was 152 cm. The baby's height, weight, and serum creatinine value (Scr) were 50.2 cm, 2852 g, and 0.88 mg/dl, respectively. After 6 days, the baby's Scr decreased to 0.41 mg/dl. The infant was not consuming the mother's milk during the observation period. The mother provided a written informed consent to measure both the mother's and the baby's serum drug concentrations and publish the results.

The Simcyp's built-in pregnant population model was used to create the pregnant Japanese model and simulate the PAL concentration in our pregnant patient. The physiological and demographic data in the Japanese population included in "Sim-Japanese" were used to recalibrate the corresponding parameters in the pregnant population. Furthermore, the "virtual twin" approach was adopted to personalize the Japanese pregnant model, and the Japanese pregnant model at zero weeks of gestation was used to simulate serum PAL after delivery for model standardization.

Effects of pregnancy: Fixed model simulation

Multiple physiological parameters are altered during pregnancy, resulting in significant changes in drug pharmacokinetics. Hepatic enzyme activity (CYP2D6 and CYP3A4), tissue volume (plasma volume, red blood cell [RBC] volume, fetoplacental volume, and adipose volume), blood flow (CO), blood binding (HSA), hematocrit and renal function (GFR) were chosen as the parameters of interest. By the end of gestation, maternal CYP2D6 and CYP3A4 activity would be three and 1.24 times greater than in the pre-pregnant state, respectively¹⁴; likewise, plasma, RBC volumes, and CO may increase by 50%, 28%, and 30%, respectively,¹⁴ whereas HSA, hematocrit, and

GFR may decrease by 31%, 38%, and 27%, respectively.¹⁴ The regression equations used to describe the change in the parameters of interest in our model during different gestation ages in weeks were based on Abduljalil et al.¹⁴ The input values for the pregnancy subsection of the Simcyp population section were modified to gain a thorough understanding of the mechanism underlying the variations in RIS and PAL dispositions between pregnant and non-pregnant subjects as well as to shed light on how pregnancy affects two pharmacologically active drugs, a parent drug and its metabolite, with two different clearance (CL) mechanisms. A fixed-parameter approach was used, in which all parameters, except for one specific parameter, were subjected to the physiological changes associated with pregnancy mentioned above. In other words, all parameters were assumed to undergo gestational changes, apart from one, which remained unaffected. These changes were implemented using a one-parameter-per-simulation approach. Finally, a combined model was developed where all parameters remained constant during the simulation.

Effects of renal function model on the neonate

For the Japanese neonate subject, the "sim-pediatric Japanese" population was applied without modification, and it was assumed that PAL was given as an i.v. bolus dosage. To evaluate the drug elimination in a neonate after birth, the observed PAL concentration in the neonate immediately after delivery (0.99 ng/ml in our case) was adopted as the reference point, which was assumed to be equivalent to the mean simulated maximum concentration (C_{\max}) after the i.v. dosing to the neonatal PBPK model. Therefore, the adopted PAL i.v. dosage was the one that yielded a C_{\max} equal to 0.99 ng/ml. This timepoint was excluded from statistical analysis and used as a reference point. In addition, the prediction accuracy, and the optimal ontogeny model for PAL CL in neonates were examined. Ten methods, comprising four maturation-based models^{17,19,20,24} and six Scr-based equations,^{18,21–23,25,26} were selected from GFR estimates approaches published in the literature (Table S5).

Model evaluation and statistical analysis

The following criteria were predetermined to assess model performance. First, visual predictive check for predicted (C_{pred}) and observed (C_{obs}) serum concentrations were used. Furthermore, the C_{pred} and areas under the plasma concentration-time curve (AUCs) of RIS and PAL

were compared with the observed values. The model was verified when the observed values were within the virtual population's 90% prediction interval (5th–95th percentile range), and the ratio of the predicted value to the observed value was within a two-fold difference.³⁷ Moreover, the C_{pred} and the respective C_{obs} were compared in GOF plots. Then, to assess the prediction bias and precision of each analyte concentration, the mean error percentage (ME) ± standard error (SE) and root mean square error (RMSE) of the C_{pred} compared with the C_{obs} were calculated using the following equations:

$$ME (\%) = 100 * \frac{1}{n} \sum_{i=1}^n \left(\frac{(\text{Simulated value, } i - \text{Observed value, } i)}{\text{Observed value, } i} \right)$$

$$RMSE (\%) = 100 * \sqrt{\frac{1}{n} \sum_{i=1}^n \left(\frac{(\text{Simulated value, } i - \text{Observed value, } i)}{\text{Observed value, } i} \right)^2}$$

RESULTS

Model development in the adult population

Figure S2 depicts the healthy volunteers' quantitative mass balance diagram for RIS and PAL after a single oral

dose of 1 mg RIS based on our PBPK model. According to the PBPK mass balance simulation, Simcyp estimated the RIS bioavailability (F) to be 59%, the fraction undergoing first-pass metabolism to be 40%, and the fraction of RIS and PAL excreted unchanged in the urine to be 4% and 44%, respectively.

Model verification in the adult population, and extrapolation to pregnant and pediatric populations

Figure 1 depicts the visual predictive check (VPC) of C_{pred} and C_{obs} profiles, demonstrating close agreement for both RIS and PAL. Moreover, 100% of the simulated AUC and C_{pred} values for RIS and PAL were within the two-fold error acceptance range, and 77.1% fell under the 1.25-fold error range. The predicted CL_t/F and CL_t values for RIS and PAL in adults were 26.5 and 65.1 L/h, respectively. Figure 2 illustrates the GOF plots of C_{pred} and their respective C_{obs} of RIS or PAL in pediatric population in the previous report.¹³ Figure 3 depicts the VPC plots of the PBPK model for AM plasma concentrations at steady-state in the pregnant population after repeated doses of 5 mg oral RIS.¹³

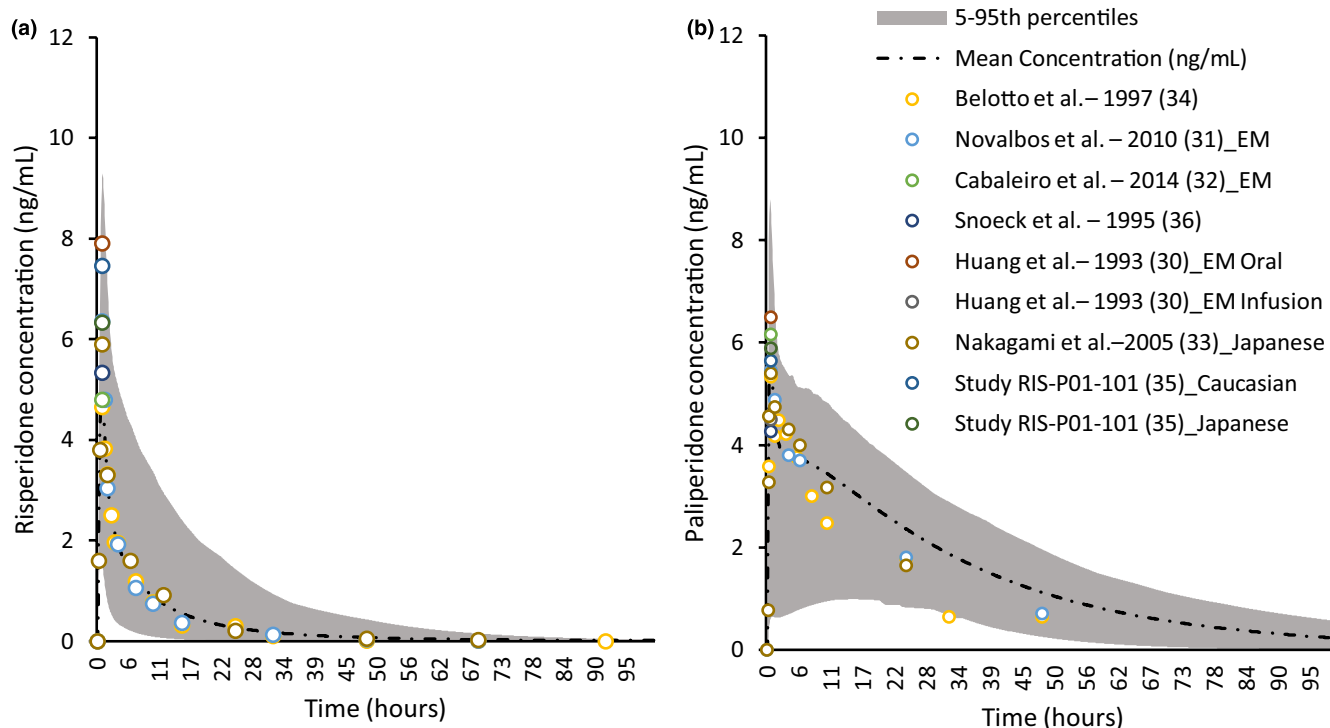


FIGURE 1 Visual predictive check of the predictions of White and Japanese healthy adult population models for RIS and PAL using observed data from seven prior clinical studies^{30–36} with nine adult datasets following a single oral dose of 1 mg risperidone. The gray area indicates the 5th–95th percentile prediction interval, and the dashed black line represents the simulated mean drug concentration. The open circles mark the actual measured concentrations. (a) PBPK simulation for RIS concentration, and (b) PBPK simulation for plasma PAL concentration. PAL, paliperidone; PBPK, physiologically-based pharmacokinetic; RIS, risperidone.

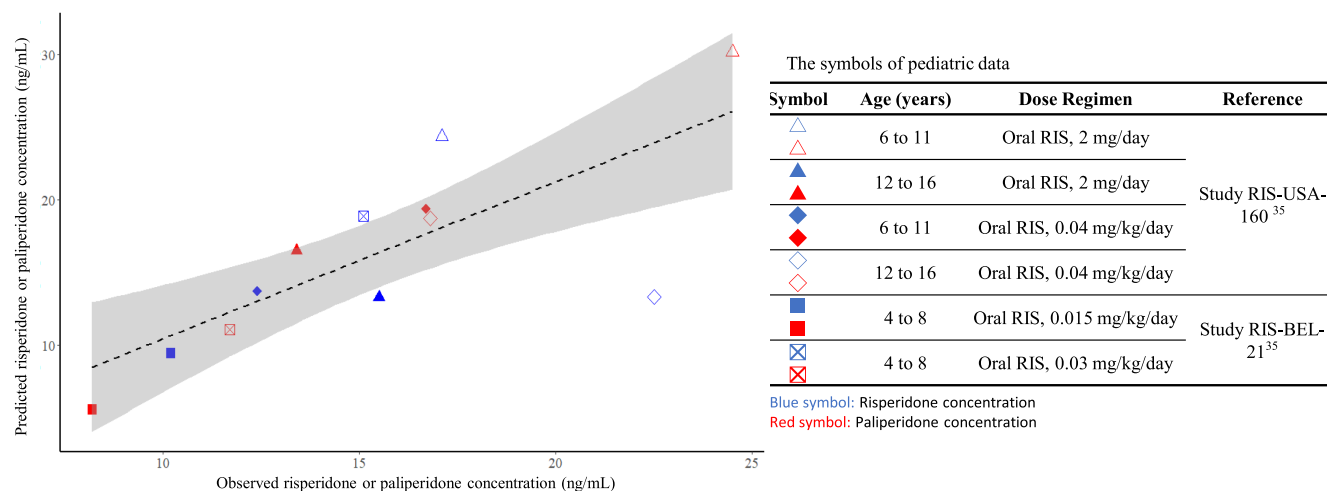


FIGURE 2 Goodness-of-fit plot of predicted versus observed concentrations of RIS and PAL maximum concentration in two previous clinical studies.³⁵ The dashed black line denotes the smooth line, whereas the light gray area denotes the prediction's 95% prediction confidence interval. Each symbol represents a single concentration–time profile, with RIS represented by blue symbols and PAL by red symbols. PAL, paliperidone; RIS, risperidone.

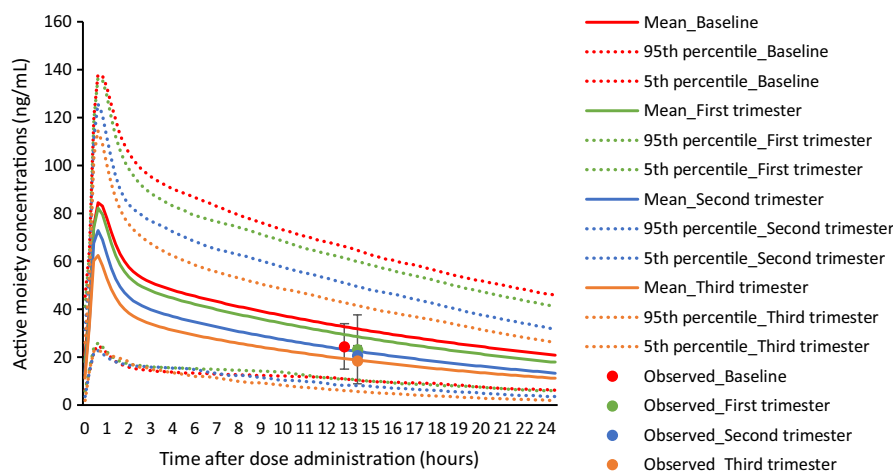


FIGURE 3 Visual predictive check of the pregnant PBPK model predictions for AM concentration using observed data from a previous clinical study in pregnant women.¹³ with nine sampling points at baseline, and five sampling points in each pregnancy trimester after a repeated oral dose of 5 mg RIS in four pregnant patients. The observed AM concentrations were detected in the first, second, and third trimesters during gestational weeks 6, 20, and 34, respectively. The lines depict the simulated mean drug concentration at the baseline (red), the first trimester (green), the second trimester (blue), and the third trimester (orange). The 5th–95th percentile prediction intervals for the baseline, the first, the second, and the third trimesters, respectively, are shown by the dashed lines. The filled circle depicts the average AM observed during steady-state after 13.3 ± 1.5 h at baseline (red) and 13.8 ± 1.6 h in the pregnant population (green, blue, and orange), with the error bars representing their 95% confidence intervals. AM, active moiety; PBPK, physiologically-based pharmacokinetic; RIS, risperidone.

Maternal serum RIS and PAL concentrations and application to the individual subject

RIS was not detected in all maternal serum samples (below 0.5 ng/ml). The serum PAL concentrations were between 2.05–3.80 ng/ml before childbirth (Figure 4a) and 3.80–9.90 ng/ml postpartum (Figure 4b). The RIS concentrations in the umbilical artery and vein were undetectable,

whereas the PAL concentrations were 1.10 and 1.05 ng/ml in the umbilical artery and vein, respectively. The median PAL maternal-to-cord concentration ratio was calculated to be 2.83 (range 1.98–3.61). All observed maternal serum concentrations before and after delivery fell within the 5th–95th percentile prediction interval of the virtual population generated by the Simcyp simulator.

Table 1 summarizes the changes in RIS and PAL pharmacokinetic parameters throughout the gestation period

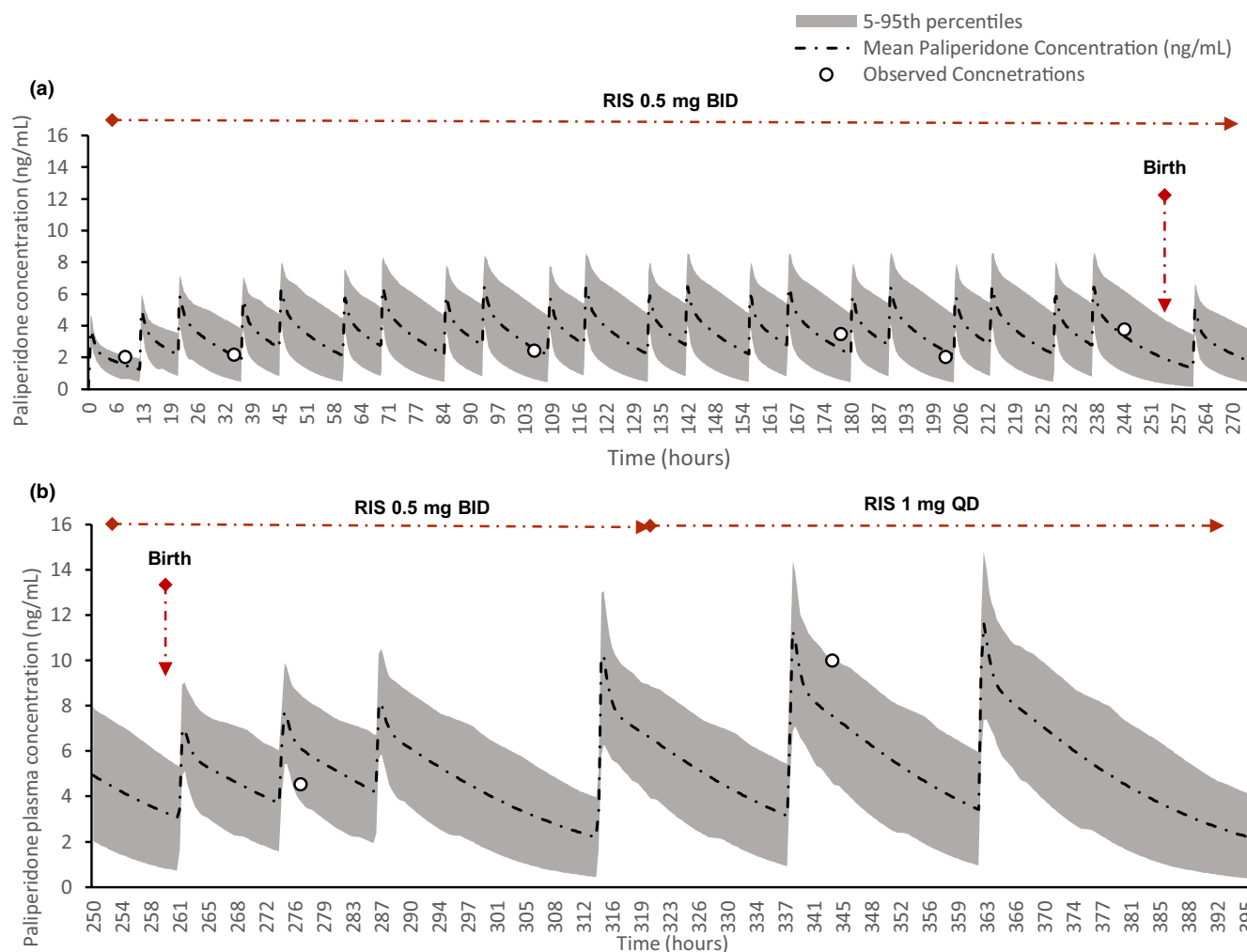


FIGURE 4 A visual predictive check of the ability of the customized PBPK model to describe PAL concentrations after oral administration of RIS 0.5 mg twice daily in a Japanese pregnant patient before and after delivery. (a) PBPK simulation for maternal PAL concentration in a pregnant Japanese woman, and (b) post-delivery maternal PBPK simulation up to day 4 postpartum utilizing “pregnancy” parameters at zero weeks’ gestation. Open circles represent the observed concentrations plotted across time, the dash-dotted line is the mean of the simulated PAL concentrations, and the gray area indicates the 5th–95th percentile prediction interval. PAL, paliperidone; PBPK, physiologically-based pharmacokinetic; RIS, risperidone.

as predicted by our PBPK model. The estimated maternal hepatic clearance, renal clearance, and CL_t of RIS and PAL increased as the pregnancy progressed, whereas the F of RIS at 40 weeks decreased to half compared to 0 week (baseline; Table 1). In accordance with the Westin et al. study,¹³ a fixed-parameter approach was used to deduce the mechanisms behind the observed variations in RIS and PAL serum levels between pregnant and pre-pregnant subjects captured by our PBPK model. The CYP2D6 enzyme, CYP3A4 enzyme, serum albumin, hematocrit, tissue volumes, cardiac output, and GFR were chosen as the parameters of interest in our model to explain the observed decrease in RIS and PAL serum concentrations during pregnancy. As demonstrated in Table 2, the RIS CL_t in the CYP2D6-parameter fixed scenario was the lowest, and serum albumin and hematocrit were associated with changes in RIS CL_t during pregnancy, but

to a lower extent compared to CYP2D6. At the same time, changes in CYP3A4 activity, volumes of plasma, RBCs, adipose, fetoplacental, cardiac output, and GFR had a negligible effect on the CL_t of RIS. CYP2D6 activity, serum albumin, fetoplacental volume, and GFR had a modest effect on PAL C_{max} , whereas other parameters had almost no effects. In the combined model, where all parameters were fixed, the CL_t of RIS and the predicted PAL C_{max} were comparable to the values obtained by the non-pregnant model (zero weeks).

Neonate serum PAL concentrations and application to the individual subject

RIS was not detected in the neonatal serum samples (below 0.5 ng/mL). The neonate serum PAL

TABLE 1 Mean predicted values of RIS and PAL pharmacokinetic parameters following oral RIS dosing in pregnant virtual patients throughout the gestational period

Parameters of comparison		Gestation of pregnancy				Fold change (0 vs. 40 weeks)
		0 week	10 weeks	20 weeks	30 weeks	40 weeks
Risperidone	Absorption					
	F_a	0.99	0.99	0.99	0.99	0.99
	F_g	0.99	0.99	0.99	0.99	0.98
	F_h	0.53	0.47	0.40	0.33	0.27
Distribution	F	0.52	0.46	0.39	0.33	0.26
	V_{ss} (L/kg)	1.96	1.97	1.99	2.01	2.06
	F_{up}	0.16	0.17	0.18	0.19	0.21
	B/P ratio	0.72	0.73	0.74	0.75	0.76
Elimination	f_m and excretion					
		82.7	84.4	86.5	88.5	90.1
	CYP2D6 (%)	3.4	3.3	3.2	3.1	3.1
	CYP3A4 (%)	9.8	8.1	6.3	4.9	3.9
	Additional HLM (%)	4.1	4.3	4.0	3.5	2.9
	Renal (%)	74	76	77	77	80
	Q_h (L/h)	381	485	656	894	1198
	CYP2D6 CL_{int} (L/h)	9	11	14	18	22
	CYP3A4 CL_{int} (L/h)	26	26	26	26	26
	Unidentified Hepatic CL_{int} (L/h)	416	522	696	937	1246
Paliperidone	Hepatic CL_{int} (L/h)	26.2	29.4	33.6	38.1	42.6
	CL_h (L/h)	0.92	1.11	1.21	1.23	1.15
	CL_r (L/h)	27.1	30.6	34.9	39.4	43.8
	CL_t (L/h)	8.8	11.2	15.1	20.6	27.6
	CYP2D6 CL_{int} (L/h)	2.9	2.9	2.9	2.9	2.9
	Unidentified Hepatic CL_{int} (L/h)	11.7	14.1	18.0	23.5	30.5
	Hepatic CL_{int} (L/h)	2.54	3.13	4.12	5.55	7.51
	CL_h (L/h)	3.60	4.35	4.75	4.81	4.53
	CL_r (L/h) ^a	6.14	7.48	8.87	10.4	12.0
	CL_t (L/h) ^a	59	58	54	46	38
Paliperidone	Fraction excreted in urine (%)					
		8.8	11.2	15.1	20.6	27.6
	CYP2D6 CL_{int} (L/h)	2.9	2.9	2.9	2.9	2.9
	Unidentified Hepatic CL_{int} (L/h)	11.7	14.1	18.0	23.5	30.5
	Hepatic CL_{int} (L/h)	2.54	3.13	4.12	5.55	7.51
	CL_h (L/h)	3.60	4.35	4.75	4.81	4.53
	CL_r (L/h) ^a	6.14	7.48	8.87	10.4	12.0
	CL_t (L/h) ^a	59	58	54	46	38
	Fraction excreted in urine (%)					
		8.8	11.2	15.1	20.6	27.6

Note: Fold change: 40-week gestational value was divided by zero-week gestational value.

Abbreviations: B/P ratio, blood/plasma concentration ratio; CL_{hp} , total hepatic clearance; CL_{int} , intrinsic clearance; CL_r , renal clearance; CL_{up} , total drug clearance; F_a , fraction of risperidone absorbed from the gut; F_g , fraction of risperidone that escapes gut metabolism; F_h , fraction of risperidone that escapes hepatic metabolism; f_m , estimated fraction metabolized; F_{up} , unbound fraction of drugs in plasma; HLM, human liver microsomes; PAL, paliperidone; RIS, risperidone; Q_h , hepatic blood flow; V_{ss} , volume of distribution at steady-state.

^aThese output values were simulated using i.v. PAL as a probe drug and pregnancy population.

TABLE 2 Model predictions for total plasma RIS clearance and PAL maximum plasma concentrations in a 40-week customized Japanese pregnant PBPK model with a dose of 0.5 mg RIS twice daily and the fixed-parameter technique

Population model			RIS		PAL	
			CL _t (L/h)	Fold change ^b	C _{max} (ng/ml)	Fold change ^b
Basic pregnant model (0 week)			27.1	(0.62)	7.05	(1.40)
Basic pregnant model (40 weeks)			43.8	(Ref)	5.03	(Ref)
Fixed-parameter model	Enzymes	CYP2D6	31.8	(0.73)	5.51	(1.09)
		CYP3A4	43.5	(0.99)	4.99	(0.99)
	Blood binding	Serum albumin (g/L)	40.9	(0.93)	5.51	(1.09)
		Hematocrit %	41.9	(0.96)	5.05	(1.00)
	Tissue volumes	Plasma volume (L)	43.8	(1.00)	5.06	(1.01)
		RBCs volume (L)	43.8	(1.00)	5.03	(1.00)
		Adipose volume (L)	43.8	(1.00)	5.02	(1.00)
		Fetoplacental volume (L)	43.8	(1.00)	5.55	(1.10)
	Blood flows	Cardiac output (L/h)	43.8	(1.00)	5.27	(1.05)
	Renal function	GFR (ml/min)	43.5	(0.99)	5.41	(1.08)
	Combined ^a		27.5	(0.63)	7.08	(1.41)

Abbreviations: CL_t, total drug clearance; CL_{int}, intrinsic clearance; C_{max}, maximum drug plasma concentration; GFR, glomerular filtration rate; PAL, paliperidone; RBCs, red blood cells; RIS, risperidone.

^aAll parameters of interest were fixed in the combined model.

^bIn fold change calculations, the gestational 40 weeks was used as the base value.

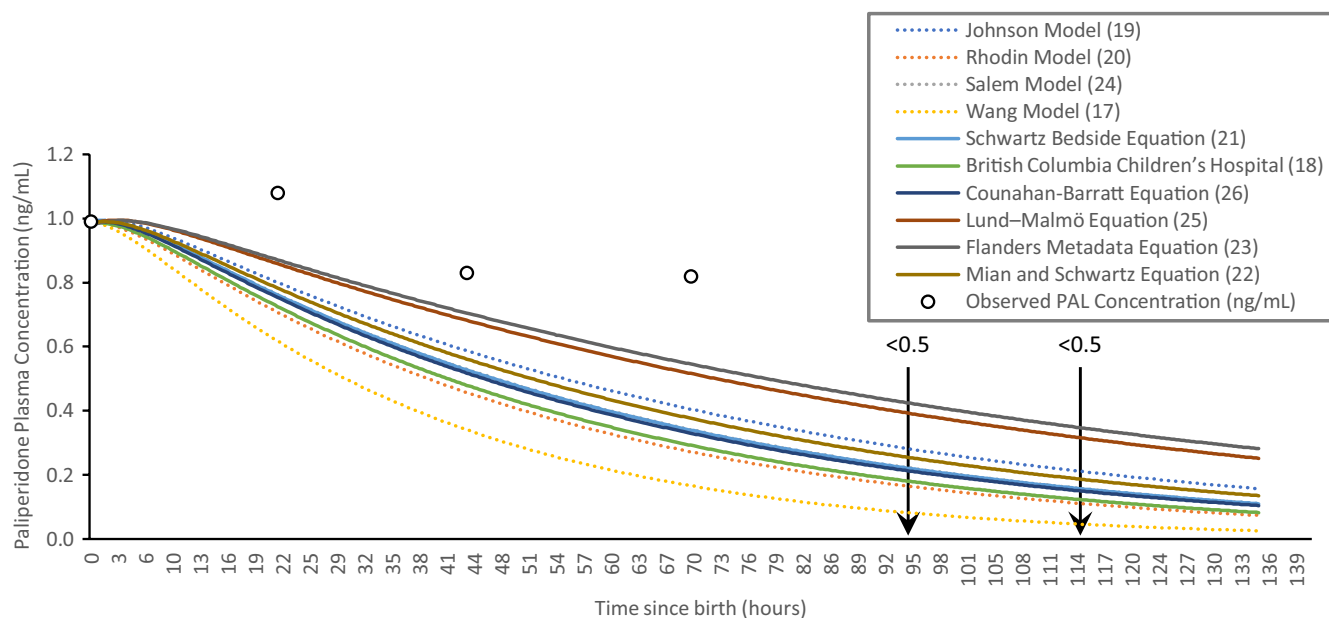


FIGURE 5 A visual predictive check of the tailored PBPK model's ability to estimate GFR in a Japanese neonate utilizing paliperidone as a probe drug and a "pediatric" population using 10 different GFR estimation methods. PAL was apparently given as an IV bolus at a dose that resulted in a paliperidone concentration of 0.99 ng/mL, the observed concentration right after birth that was used as a benchmark. The open circles indicate actual PAL concentrations. GFR, glomerular filtration rate; PAL, paliperidone; PBPK, physiologically-based pharmacokinetic; RIS, risperidone.

concentrations were 0.99, 1.03, 0.83, and 0.82 ng/mL on 0, 1, 2, and 3 days after birth, respectively, and became undetectable afterward (Figure 5). Table S5 summarizes our study's selected renal maturation models and SCR-based equations, and the ME% and RMSE% values for

PAL concentrations calculated using all chosen GFR estimation methods, with the first timepoint was excluded from the ME% and RMSE% calculation as it was used as a reference point. Among the 10 equations used to investigate the accuracy of different eGFR methods, two

Scr-based equations (Flanders metadata²³ and Lund-Malmö²⁵) and one maturation-based model (Simcyp default model¹⁹) generated the most accurate results using our Japanese neonatal PBPK model.

DISCUSSION

Aside from serum concentrations, no previous research has performed a quantitative pharmacokinetic analysis of RIS and PAL throughout pregnancy. Moreover, assessments of RIS and PAL concentrations in pregnant women and neonates are limited, primarily due to the absence of a suitable safety profile for RIS in such cases. According to the Australian categorization system for prescribing medicines in pregnancy,³⁸ RIS is a C category drug, implying that it may cause or is suspected of causing harm to the human fetus or neonate with no malformations.³⁸

RIS is an intermediate hepatic extraction drug with a bioavailability of 70% (CV = 25%) when administered orally.^{28,39} The hepatic route is responsible for ~95% of total RIS metabolism, with $41.3 \pm 7.0\%$ (SD) of the RIS dosage undergoing first-pass metabolism.³⁹ In contrast, urinary excretion only accounts for a small portion of RIS elimination ($3.4 \pm 2.6\%$ [SD])³⁰ and a substantial portion of its active metabolite PAL elimination ($59.4 \pm 7.1\%$ [SD]).¹⁰ Using the Simcyp V21's mass balance output option, we could accurately report RIS elimination mass balance after a single 1 mg RIS dose in healthy volunteers (Figure S2). RIS bioavailability, the percentage of RIS metabolized through first-pass metabolism, and the fractions of RIS and PAL excreted unchanged in the urine were predicted to be 59%, 40%, 4%, and 44%, respectively. These alignments between the observed and the predicted values added an extra validation layer for our RIS and PAL PBPK models, which is essential for maximizing the validity of the PBPK model-informed approach to precision dosing across populations.⁴⁰ The estimated CL_t and CL_t/F values of RIS in adults were 26.5 and 65.1 L/h, respectively, which were comparable to the mean reported values (23.6 and 65.4 L/h, respectively) in healthy volunteers.^{30,39} Similarly, the predicted PAL CL_t value of 5.19 L/h was the same as the average observed value (5.19 L/h) in literature.^{10,30} Scaling the adult PBPK model to children and pregnant women confirms the capacity of PBPK to predict pharmacokinetics in specific populations. Moreover, we demonstrated the utility of using an individualized PBPK model to explain the differences in pharmacokinetic parameters between pregnant and non-pregnant subjects.

Westin et al.¹³ retrospectively monitored the effects of eight antipsychotic drugs, including RIS, in 110 pregnancies. Notwithstanding their small sample size for RIS, an inverse relationship between the AM serum

concentrations and gestation age was depicted, with the AM concentrations decreasing from 24.4 ng/ml at the baseline to 18.4 ng/ml in the third trimester,¹³ as shown in Figure 3. During pregnancy, changes in oral bioavailability, tissue volumes, blood bindings, enzyme activity, and cardiac output could theoretically cause this observed decrease in the AM concentration throughout pregnancy. In our case, the maternal RIS concentrations were not detected in all samples, and the PAL concentrations seemed to increase after birth, although the dosage of RIS was changed from 0.5 mg twice a day to 1 mg once a day (Figure 4). In our PBPK analysis, at the end of pregnancy, CL_{int} of RIS and PAL mediated by CYP2D6 were three times higher than in the non-pregnant state, and CL_t of both drugs were increased 1.61 and 1.95-times, respectively (Table 1). Additionally, our model predicted a decline in the F of RIS from 0.52 at 0 weeks to 0.26 at 40 weeks. This decline was primarily attributable to a reduction in the RIS fraction that escaped hepatic metabolism (F_h) from 0.53 to 0.27 near the end of the gestation period. In contrast, the fraction of RIS that escaped gut metabolism (F_g) and the fraction of RIS absorbed from the gut (F_a) remained nearly unchanged during pregnancy, and both values were as high as 0.99. Although hepatic CYP2D6 induction during pregnancy promotes PAL production through RIS 9-hydroxylation, the increased CL_t of PAL nullified the increase in PAL concentrations. Actually, in the fixed-parameter combined model, where all the parameters of interest were held constant, the predicted PAL C_{max} as well as RIS CL_t were almost equal to the values observed in the non-pregnant state (Table 2). Namely, the decreased serum albumin and the increased fetoplacental volume, GFR, and CYP2D6 activity, with a concomitant increase in PAL production from RIS hepatic metabolism, influenced RIS and PAL pharmacokinetics during pregnancy.

Pregnant women had a two-fold increase in PAL CL_t compared to non-pregnant women. Toward the end of pregnancy, only 38% of PAL had been excreted in the urine, compared to 59% in the basic model (Table 1). Interestingly, the increase in CYP2D6 activity during pregnancy was sufficient for the primary route of PAL elimination that practically enabled the transition from renal to metabolic. These results support that the primary route of clonidine clearance shifts from the kidneys to drug-metabolizing organs during pregnancy.⁴¹ We believe that these findings have increased our understanding on the complexity of RIS and PAL disposition during pregnancy.

In our study, we attempted to calculate the maternal-to-cord concentration ratio for PAL which is considered as a useful in vivo index of relative intrauterine drug exposure that has been utilized in previous studies.^{42–44} Assessment of the fetal drug exposure may aid in directing treatment

selection, providing a greater insight into the extent to which intrauterine drug exposure is primarily responsible for neonatal complications.⁴³ In a previous case report of a pregnant woman on PAL depot, the concentration of PAL in the umbilical vein was approximately half of the maternal concentrations (7.3 ng/ml vs. 13.85 ± 1.62 [SD] ng/ml, respectively), indicating appreciable fetal exposure to the drug at steady-state.⁴⁵ In our study, the median PAL maternal-to-cord concentration ratio was determined to be 2.83 (range 1.98–3.61) at steady-state (typically after 4–5 days for PAL²⁸), which corresponds reasonably well with their findings. In another previous study,⁴³ the maternal-to-cord plasma ratio for AM was determined to be 2.44 ± 2.80 (SD), which coincides to the ratio for PAL alone.

Interestingly, the PAL concentration in our newborn was approximately one-third of the maternal one, and gradually decreased after birth (Figure 5). Our neonate's Scr values (0.88 mg/dl on day 1 and 0.41 mg/dl on day 6) were consistent with the typical progression of renal function in neonates.¹⁶ Neonatal Scr reflects the mother's relatively high level of Scr (~0.74–0.79 mg/dl) at birth,¹⁶ and the Scr concentration drops with the concomitant rapid growth in GFR during the early postnatal weeks. Due to the expected poor clearance in neonates and the lack of clarity regarding which factors best reflect the GFR, we evaluated numerous GFR estimating approaches to identify the optimal ontogeny model for this vulnerable population using our personalized PBPK model. In the Simcyp software, a renal maturation function is incorporated into the pediatric population models to improve prediction accuracy, particularly for children less than 2 years old. Four maturation models and six Scr-based equations were studied (Table S5). To account for the change in anthropometric parameters with age, most GFR maturation models include a body weight variable in addition to age. Simcyp's default model is a sigmoidal maximum effect model based on the BSA model published by Johnson et al.¹⁹ Furthermore, Wang et al.¹⁷ and Salem et al.²⁴ used gestational age, postnatal age, and weight in their published maturation models. In contrast, Scr-based equations provide a more practical and extensively utilized alternative method for determining eGFR. Consequently, two Scr-based equations (Flanders metadata²³ and Lund-Malmö²⁵) and one maturation-based model (the Simcyp default model¹⁹) yielded the most accurate RMSE%, ME%, and VPC values regarding PAL plasma concentration (Table S5 and Figure 5). Llanos-Paez et al.⁴⁶ used the chromium 51-labeled ethylene diamine tetraacetic acid excretion test to compare the measured values of GFR to the GFR values estimated from 22 equations in pediatric oncology patients. Similar to our findings, the authors

determined that the Flanders metadata equation²³ had the lowest ME% and RMSE%, and demonstrated accuracy within 30% for over 75% of GFR estimates.

Our study has a number of limitations. First, to use the PBPK model approach with Scr-based equations, we used the Scr at birth because Simcyp does not have the option to account for the rapid decline in Scr during the first days of life in the pediatric ontogeny. Therefore, the superior performance of Scr-based equations over maturation models should be interpreted with caution. Second, the presence of only three observed PAL plasma concentrations in our study necessitates further analysis with larger number of data points. Third, we did not include the prediction of intrauterine fetal drug exposure by using PBPK pregnant model in this report, which we believe is a worthwhile topic for further research.

In conclusion, this study demonstrated the feasibility of using an individualized PBPK model to predict changes in RIS and PAL pharmacokinetics during pregnancy and neonatal periods. We believe in the value of sharing our findings to deepen the overall understanding of antipsychotic pharmacokinetics during pregnancy. Our PBPK model explained the mechanisms behind changes in RIS and PAL plasma concentrations and clearances observed in pregnant women. This model might also optimize RIS dosing regimens across populations as part of model-informed precision dosing, moving further away from a “one-size-fits-all” approach and avoiding subtherapeutic doses that could expose the mother and fetus to both the drug and the disease.

AUTHOR CONTRIBUTIONS

W.Y.B.M., K.Y., and I.Y. wrote the manuscript. W.Y.B.M., K.Y., I.Y., K.I., and T.O. designed the research. W.Y.B.M., K.Y., I.Y., T.I., N.F., K.F., T.H., I.O., and H.I. performed the research. W.Y.B.M., K.Y., I.Y., T.I., N.F., K.F., T.H., I.O., and H.I. analyzed the data.

ACKNOWLEDGMENTS

The authors would like to express our gratitude to the individuals whose data were examined in this study.

FUNDING INFORMATION

This work was supported in part by research grants from JSPS KAKENHI, Grant Number 19K07219 and 22K06697.


CONFLICT OF INTEREST

The authors declared no competing interests for this work.

DATA AVAILABILITY STATEMENT

All data generated in the current study are available from the corresponding author on reasonable request.

ORCID

Walaa Y. B. Mahdy  <https://orcid.org/0000-0002-2277-8521>

Kazuhiro Yamamoto  <https://orcid.org/0000-0002-7513-6725>

Takahiro Ito  <https://orcid.org/0000-0003-2032-4443>

Ikuko Yano  <https://orcid.org/0000-0001-9517-5628>

REFERENCES

- Huybrechts KF, Hernández-Díaz S, Paterno E, et al. Antipsychotic use in pregnancy and the risk for congenital malformations. *JAMA Psychiat*. 2016;73(9):938-946.
- Hahn-Holbrook J, Cornwell-Hinrichs T, Anaya I. Economic and health predictors of National Postpartum Depression Prevalence: a systematic review, meta-analysis, and meta-regression of 291 studies from 56 countries. *Front Psych*. 2018;8:248.
- Motrico E, Bina R, Domínguez-Salas S, et al. Impact of the Covid-19 pandemic on perinatal mental health (Riseup-PPD-COVID-19): protocol for an international prospective cohort study. *BMC Public Health*. 2021;21(1):368.
- Zhang L, Brown SJ, Shan Y, et al. CYP2D6 genetic polymorphisms and risperidone pharmacokinetics: a systematic review and meta-analysis. *Pharmacotherapy*. 2020;40(7):632-647.
- Toh S, Li Q, Cheetham TC, et al. Prevalence and trends in the use of antipsychotic medications during pregnancy in the U.S., 2001–2007: a population-based study of 585,615 deliveries. *Arch Womens Ment Health*. 2013;16(2):149-157.
- Wlodarczyk BJ, Ogle K, Lin LY, Bialer M, Finnell RH. Comparative teratogenicity analysis of valnoctamide, risperidone, and olanzapine in mice. *Bipolar Disord*. 2015;17(6):615-625.
- Betcher HK, Montiel C, Clark CT. Use of antipsychotic drugs during pregnancy. *Curr Treat Options Psychiatry*. 2019;6(1):17-31.
- Ennis ZN, Damkier P. Pregnancy exposure to olanzapine, quetiapine, risperidone, aripiprazole and risk of congenital malformations. A systematic review. *Basic Clin Pharmacol Toxicol*. 2015;116(4):315-320.
- Mannens G, Huang ML, Meuldermans W, Hendrickx J, Woestenborghs R, Heykants J. Absorption, metabolism, and excretion of risperidone in humans. *Drug Metab Dispos*. 1993;21(6):1134-1141.
- Vermeir M, Naessens I, Remmerie B, et al. Absorption, metabolism, and excretion of paliperidone, a new monoaminergic antagonist, in humans. *Drug Metab Dispos*. 2008;36(4):769-779.
- Mannens G, Meuldermans W, Snoeck E, Heykants J. Plasma protein binding of risperidone and its distribution in blood. *Psychopharmacology*. 1994;114(4):566-572.
- Syrejschchikova T, Smolina N, Kondratyuk V, Dobretsov G, Uzbekov M. Influence of antipsychotic drug risperidone on human serum albumin affinity to organic anions. *Curr Drug Discov Technol*. 2018;15(3):263-269.
- Westin AA, Brekke M, Molden E, Skogvoll E, Castberg I, Spigset O. Treatment with antipsychotics in pregnancy: changes in drug disposition. *Clin Pharmacol Ther*. 2018;103(3):477-484.
- Abduljalil K, Furness P, Johnson TN, Rostami-Hodjegan A, Soltani H. Anatomical, physiological and metabolic changes with gestational age during normal pregnancy: a database for parameters required in physiologically based pharmacokinetic modelling. *Clin Pharmacokinet*. 2012;51(6):365-396.
- Polasek TM, Rostami-Hodjegan A. Virtual twins: understanding the data required for model-informed precision dosing. *Clin Pharmacol Ther*. 2020;107(4):742-745.
- Zhang Y, Mehta N, Muhari-Stark E, Burckart GJ, Anker J, Wang J. Pediatric renal ontogeny and applications in drug development. *J Clin Pharmacol*. 2019;59(S1):S9-S20. doi:10.1002/jcph.1490
- Wang J, Kumar SS, Sherwin CM, et al. Renal clearance in newborns and infants: predictive performance of population-based modeling for drug development. *Clin Pharmacol Ther*. 2019;105(6):1462-1470.
- Mattman A, Eintracht S, Mock T, et al. Estimating pediatric glomerular filtration rates in the era of chronic kidney disease staging. *J Am Soc Nephrol*. 2006;17(2):487-496.
- Johnson TN, Rostami-Hodjegan A, Tucker GT. Prediction of the clearance of eleven drugs and associated variability in neonates, infants and children. *Clin Pharmacokinet*. 2006;45(9):931-956.
- Rhodin MM, Anderson BJ, Peters AM, et al. Human renal function maturation: a quantitative description using weight and postmenstrual age. *Pediatr Nephrol*. 2009;24(1):67-76.
- Schwartz GJ, Work DF. Measurement and estimation of GFR in children and adolescents. *Clin J Am Soc Nephrol*. 2009;4(11):1832-1843.
- Mian AN, Schwartz GJ. Measurement and estimation of glomerular filtration rate in children. *Adv Chronic Kidney Dis*. 2017;24(6):348-356.
- Pottel H, Mottaghy FM, Zaman Z, Martens F. On the relationship between glomerular filtration rate and serum creatinine in children. *Pediatr Nephrol*. 2010;25(5):927-934.
- Salem F, Johnson TN, Hodgkinson ABJ, Ogungbenro K, Rostami-Hodjegan A. Does “birth” as an event impact maturation trajectory of renal clearance via glomerular filtration? Reexamining data in preterm and full-term neonates by avoiding the creatinine bias. *J Clin Pharmacol*. 2021;61(2):159-171.
- Björk J, Bäck S-E, Sterner G, et al. Prediction of relative glomerular filtration rate in adults: new improved equations based on Swedish Caucasians and standardized plasma-creatinine assays. *Scand J Clin Lab Invest*. 2007;67(7):678-695.
- Counahan R, Chantler C, Ghazali S, Kirkwood B, Rose F, Barratt TM. Estimation of glomerular filtration rate from plasma creatinine concentration in children. *Arch Dis Child*. 1976;51(11):875-878.
- WebPlotDigitizer – Copyright 2010–2021 Ankit Rohatgi. Cited March 22, 2022. <https://apps.automeris.io/wpd/>
- PubChem. Risperidone. Cited October 13, 2021. <https://pubchem.ncbi.nlm.nih.gov/compound/5073>
- PubChem. Paliperidone. Cited March 22, 2022. <https://pubchem.ncbi.nlm.nih.gov/compound/115237>
- Huang M-L, Peer AV, Woestenborghs R, et al. Pharmacokinetics of the novel antipsychotic agent risperidone and the prolactin response in healthy subjects. *Clin Pharmacol Ther*. 1993;54(3):257-268.
- Novalbos J, López-Rodríguez R, Román M, Gallego-Sandín S, Ochoa D, Abad-Santos F. Effects of CYP2D6 genotype on the pharmacokinetics, pharmacodynamics, and safety of risperidone in healthy volunteers. *J Clin Psychopharmacol*. 2010;30(5):504-511.

32. Cabaleiro T, Ochoa D, López-Rodríguez R, et al. Effect of polymorphisms on the pharmacokinetics, pharmacodynamics, and safety of risperidone in healthy volunteers. *Hum Psychopharmacol*. 2014;29(5):459-469.
33. Nakagami T, Yasuifurukori N, Saito M, Tateishi T, Kaneo S. Effect of verapamil on pharmacokinetics and pharmacodynamics of risperidone: In vivo evidence of involvement of P-glycoprotein in risperidone disposition. *Clin Pharmacol Ther*. 2005;78(1):43-51.
34. Belotto KCR, Raposo NRB, Ferreira AS, Gattaz WF. Relative bioavailability of two oral formulations of risperidone 2 mg: a single-dose, randomized-sequence, open-label, two-period crossover comparison in healthy Brazilian volunteers. *Clin Ther*. 2010;32(12):2106-2115.
35. Janssen Pharmaceutical K.K. *Report on the Deliberation Results*. Janssen Pharmaceutical K.K; 2016.
36. Snoeck E, Van Peer A, Mannens G, et al. Influence of age, renal and liver impairment on the pharmacokinetics of risperidone in man. *Psychopharmacology*. 1995;122(3):223-229.
37. Cui C, Sia JEV, Tu S, et al. Development of a physiologically based pharmacokinetic (PBPK) population model for Chinese elderly subjects. *Br J Clin Pharmacol*. 2021;87(7):2711-2722.
38. Administration AGD of HTG. Prescribing medicines in pregnancy database. Therapeutic goods administration (TGA). Australian government department of Health; 2021. Cited February 13, 2022. <https://www.tga.gov.au/prescribing-medicines-pregnancy-database>
39. Vermeulen A, Piotrovsky V, Ludwig EA. Population pharmacokinetics of risperidone and 9-Hydroxyrisperidone in patients with acute episodes associated with bipolar I disorder. *J Pharmacokinet Pharmacodyn*. 2007;34(2):183-206.
40. Rowland Yeo K, Venkatakrishnan K. Physiologically-based pharmacokinetic models as enablers of precision dosing in drug development: pivotal role of the human mass balance study. *Clin Pharmacol Ther*. 2021;109(1):51-54.
41. Buchanan ML, Easterling TR, Carr DB, et al. Clonidine pharmacokinetics in pregnancy. *Drug Metab Dispos*. 2009;37(4):702-705.
42. McConnell C, Thoene M, Van Ormer M, et al. Plasma concentrations and maternal-umbilical cord plasma ratios of the six Most prevalent carotenoids across five groups of birth gestational age. *Antioxidants*. 2021;10(9):1409.
43. Newport DJ, Calamaras MR, DeVane CL, Donovan J. Atypical antipsychotic administration during late pregnancy: placental passage and obstetrical outcomes. *Am J Psychiatry*. 2007;164(8):1214-1220.
44. Lancz K, Palkovičová L, Patayová H, et al. Ratio of cord to maternal serum PCB concentrations in relation to their congener-specific physicochemical properties. *Int J Hyg Environ Health*. 2015;218(1):91-98.
45. Binns R, O'Halloran SJ, Teoh S, Doherty K, Joyce DA. Placental transfer of paliperidone during treatment with a depot formulation. *J Clin Psychopharmacol*. 2017;37(4):474-475.
46. Llanos-Paez CC, Staatz C, Lawson R, Hennig S. Comparison of methods to estimate glomerular filtration rate in paediatric oncology patients. *J Paediatr Child Health*. 2018;54(2):141-147.

SUPPORTING INFORMATION

Additional supporting information can be found online in the Supporting Information section at the end of this article.

How to cite this article: Mahdy WYB, Yamamoto K, Ito T, et al. Physiologically-based pharmacokinetic model to investigate the effect of pregnancy on risperidone and paliperidone pharmacokinetics: Application to a pregnant woman and her neonate. *Clin Transl Sci*. 2023;16: 618-630. doi:[10.1111/cts.13473](https://doi.org/10.1111/cts.13473)